

Effects of Preferential Solvation Revealed by Time-Resolved Magnetic Field Effects

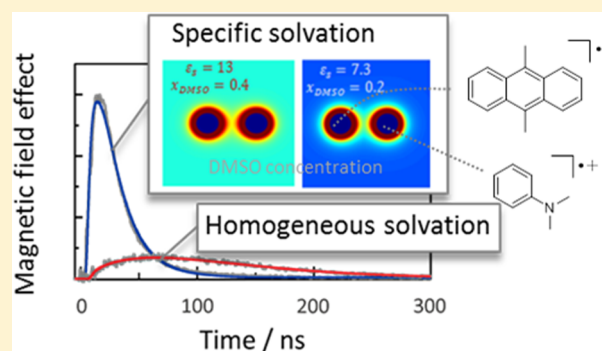
Van Thi Bich Pham,[†] Hao Minh Hoang,^{†,‡} Günter Grampp,[†] and Daniel R. Kattinig^{*,§}

[†]Institute of Physical and Theoretical Chemistry, Graz University of Technology, Stremayrgasse 9/I, A-8010 Graz, Austria

[‡]Ho Chi Minh City University of Technology and Education, Vo Van Ngan 01, Linh Chieu Ward, Thu Duc District, Ho Chi Minh City, Vietnam

[§]Physical and Theoretical Chemistry Laboratory, University of Oxford, South Parks Road, Oxford OX1 3QZ, U.K.

ABSTRACT: External magnetic fields can impact recombination yields of photoinduced electron transfer reactions by affecting the spin dynamics in transient, spin-correlated radical pair intermediates. For exciplex-forming donor–acceptor systems, this magnetic field effect (MFE) can be investigated sensitively by studying the delayed recombination fluorescence. Here, we investigate the effect of preferential solvation in microheterogeneous solvent mixtures on the radical pair dynamics of the system 9,10-dimethylantracene (fluorophore)/*N,N*-dimethylaniline (quencher) by means of time-resolved magnetic field effect (TR-MFE) measurements, wherein the exciplex emission is recorded in the absence and the presence of an external magnetic field using time-correlated single photon counting (TCSPC). In microheterogeneous environments, the MFE of the exciplex emission occurs on a faster time scale than in iso-dielectric homogeneous solvents. In addition, the local polarity reported by the exciplex is enhanced compared to homogeneous solvent mixtures of the same macroscopic permittivity. Detailed analyses of the TR-MFE reveal that the quenching reaction directly yielding the radical ion pair is favored in microheterogeneous environments. This is in stark contrast to homogeneous media, for which the MFE predominantly involves direct formation of the exciplex, its subsequent dissociation to the magneto-sensitive radical pair, and re-encounters. These observations provide evidence for polar microdomains and enhanced caging, which are shown to have a significant impact on the reaction dynamics in microheterogeneous binary solvents.



I. INTRODUCTION

Solvent polarity strongly affects the mechanism of photoinduced electron transfer (ET) reactions. In polar solvents, the process usually involves complete ET from the electron donor to the acceptor, thereby forming spin-correlated radical ion pairs (RIPs). In nonpolar solvents, the formation of excited-state charge transfer complexes, so-called exciplexes, is often observed. Expectedly, in moderately polar solvents, both quenching reactions may contribute simultaneously and radical ions can result from direct ET as well as dissociation of the exciplex.^{1–8} Due to similar spectral footprints of ion pairs and exciplexes, it is generally difficult to elaborate which channel dominates.^{9–12} The magnetic field effect (MFE) on the exciplex emission provides a versatile tool for the study of this intricate dynamics. The approach has been applied to homogeneous solvents as well as under conditions of preferential solvation, which often occur in binary solvent mixtures of vastly different polarity.^{13–18} The term “preferential solvation” subsumes nonspecific and specific interactions of solutes with specific components of binary solvent mixtures. It often induces microheterogeneity in the solvent, which is characterized by the spatially nonuniform distribution of the solvent components in the vicinity of polar

or ionic solutes. These microclusters of polar solvent molecules have a pronounced effect on the mutual diffusion and reactivity of radical ion pairs and, thus, the MFEs they elicit. So far, microheterogeneous solvation has only been studied by steady-state MFE measurements.^{16,19,20} This severely limits the insights in the radical pair dynamics in these systems, because only time-resolved MFE measurements allow one to discriminate the initial reaction products.^{1,2}

The MFE relevant to this study results from the *radical pair mechanism*. In short, the overall singlet and triplet states of the radical pair are coherently interconverted by the hyperfine interactions (HFIs) of the magnetic nuclei of the radicals.^{21–25} An external magnetic field will remove the degeneracy of the three electronic triplet sublevels (T_0 and T_{\pm}) of the spin-correlated pair (in the absence of significant exchange or electron–electron dipolar coupling). When the energy separation between these states exceeds the size of the mixing interactions, T_{\pm} cannot mix with the singlet state S . In this way, the external magnetic field reduces the probability of

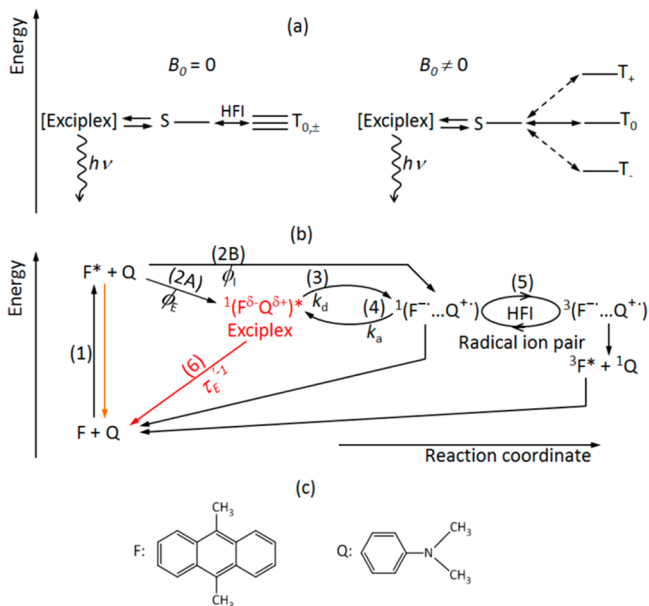
Received: January 17, 2017

Revised: March 3, 2017

Published: March 6, 2017

intersystem crossing in the radical pair and, thus, alters the relative concentrations of singlet and triplet reaction products (see Scheme 1a).^{26–28} The hyperfine-induced spin mixing

Scheme 1. (a) Illustration of the Origin of the MFE Detected via the Exciplex Emission;^a (b) Important Reaction Pathways of the Transient Species Involved in the MFE of the Exciplex;^b (c) Chemical Structures of the Fluorophore and the Donor



^aIn the absence of an external magnetic field ($B_0 = 0$), the singlet (S) and all three triplet ($T_{0,\pm}$) states are interconverted by the radical hyperfine interactions (HFI). In the presence of a sufficiently large magnetic field B_0 , the T_{\pm} states cannot mix with the S state. ^bThe red and orange arrows refer to the radiative processes of the exciplex and the locally excited fluorophore emissions, respectively.

between S and T_0 and T_{\pm} can only efficiently proceed when the electron exchange interaction, which energetically splits the S from the T-states, is smaller in magnitude than the hyperfine interactions. Owing to the fact that the electron exchange interaction depends exponentially on the distance between the radical ions, this implies that only diffusively separated radical ions can undergo S/T-conversion. Eventually, the singlet RIP concentration can be detected through the emission of the exciplex, which is produced by singlet RIP cage recombination (see Scheme 1b).^{19,20,29–33}

As a consequence of this mechanism, any factor influencing the RIP molecular dynamics may affect MFE features such as the magnitude of the MFE observed under saturating field conditions and the $B_{1/2}$ value, which gives the field intensity delivering half the saturation MFE. In this way, the exciplex system can serve as a magneto-fluorescent probe, sensitive to the local dielectric heterogeneities of binary solvents. Indeed, using magnetic-field-affected-reaction-yield (MARY) line broadening measurements, the $B_{1/2}$ values were found to vary strongly with the solvent composition in microheterogeneous solvents.^{19,20} Solvent mixtures composed of toluene (TO) and dimethyl sulfoxide (DMSO) have been studied in detail.^{15,34} Studies of the magnetic isotope effect revealed no direct transfer of spin density on solvent molecules.²⁰ Instead, the observed effects were entirely due to the radical pair dynamics.

In general, the RP lifetime is reduced in the microheterogeneous TO/DMSO environment due to an enhanced cage-effect facilitating RP reencounters. As the DMSO concentration and thus the relative macroscopic permittivity, ϵ_s , is increased, the lifetime of the RIP increases due to a smaller depth of the dielectric traps. This is a consequence of the RIPs evading swift recombination by their diffusive escape from the trap. Accordingly, the extrapolated $B_{1/2}$ values in the limit of zero donor concentration, $B_{1/2}(0)$, are larger than expected for long-lived RPs but decrease with increasing macroscopic dielectric constant, in contrast to what is seen in homogeneous solvents.²⁰ Nath and co-workers have recently suggested that two populations of exciplexes exist for the pyrene/*N,N*-dimethylaniline donor–acceptor system in comparably polar THF/DMF and benzene/acetonitrile solvent mixtures.^{35,36} The authors argue that the effect is attributed to (incomplete) relaxation of the solvent shell surrounding the contact ion pair.

The aforementioned steady-state approaches usually do not take the exciplex kinetics into account. The mechanism of fluorescence quenching by electron transfer is, however, ambiguous; i.e., the initial quenching products are a RIP via distant ET (pathway 2B of Scheme 1b) or the exciplex (pathway 2A). Several studies have illustrated the use of time-resolved MFEs of the exciplex to identify the initial quenching products in homogeneous solvents and solvent mixtures.^{1,2} In this work, we describe the solvent polarity dependence of the time-resolved MFE in homogeneous and micro-heterogeneous binary solvent mixtures as measured by time-correlated single photon counting (TCSPC). The well-studied donor–acceptor system *N,N*-dimethylaniline (quencher)/9,10-dimethylanthracene (fluorophore) serves as a magnetosensitive probe (see Scheme 1c).^{1,2,19,20,31,32} Our study gives detailed insights into the peculiar RP dynamics in microheterogeneous solvents. Throughout this work, we use the terms “preferential solvation” and “microheterogeneous medium” interchangeably, although, strictly speaking, the former refers to specific and nonspecific solute–solvent interactions, while the latter signifies the nonuniform solvent structure, which the former induce. In the present context, this semantic distinction is immaterial.

II. EXPERIMENTAL SECTION

Sample and Solvent Preparation. 9,10-Dimethylanthracene (DMAnt, Aldrich 99%) was used as received. *N,N*-Dimethylaniline (DMA, Aldrich 99.5%) was distilled under reduced pressure and subsequently handled under an argon atmosphere. The concentration of the fluorophore was constant at 1.5×10^{-5} M, while that of the quencher was 0.06 M. Solutions were prepared in septa-sealed fused silica cuvettes. All solutions were purged with solvent-saturated nitrogen gas for 15 min to remove dissolved oxygen before adding the quencher through the septum using Hamilton syringes. A series of solvent mixtures of propyl acetate (PA, Aldrich 99.5%, distilled under reduced pressure, $\epsilon_s = 6$); this and all subsequently reported values refer to a temperature of 295 K) and butyronitrile (BN, Fluka 99%, distilled under reduced pressure, $\epsilon_s = 24.7$) and of toluene (TO, Fluka 99%, distilled under reduced pressure, $\epsilon_s = 2.38$) and dimethyl sulfoxide (DMSO, Aldrich 99.9%, used as received, $\epsilon_s = 46.4$) with widely varying dielectric constants, ϵ_s , were prepared. The dielectric constants of these mixtures are given by eq 1 and eq 2 for the PA/BN and TO/DMSO systems, respectively (at 295 K):^{1,2,19,20}

$$\epsilon_s = w_{\text{PA}}\epsilon_{\text{PA}} + (1 - w_{\text{PA}})\epsilon_{\text{BN}} \quad (1)$$

$$\epsilon_s = 62.5 \exp \left[-\frac{(1 - x_{\text{DMSO}})}{0.78} \right] - 15.6 \quad (2)$$

Here, w_{PA} is the mass fraction of PA and x_{DMSO} is the mole fraction of DMSO. The homogeneous mixtures of PA/BN allow systematic variation of the solvent dielectric constants within a range of 6–24.7 (at 295 K) while keeping the viscosity (η) and the refractive index (n) almost constant. The Pekar factor, $\gamma = (1/\epsilon_\infty - 1/\epsilon_s) \approx (1/n^2 - 1/\epsilon_s)$, which governs the outer-sphere electron transfer reorganization energy, increases only moderately with increasing permittivity.^{1,2,20,37,38} For the microheterogeneous mixtures of TO/DMSO, the solvent dielectric constant was varied from 4.3 to 15.5. The viscosity and the bulk Pekar factor γ of TO/DMSO mixtures slightly increase with increasing DMSO concentration.²⁰ We are not aware of a microheterogeneous solvent mixture for which this could be avoided.

Steady-State MFE Measurements. Using the experimental setup described in ref 32, the exciplex emission was recorded at 550 nm under continuous excitation of the sample at 374 nm. For each sample, the fluorescence intensities were acquired three times under conditions of zero and saturating magnetic field exposition for 60 s each. Field-on and field-off measurements were recorded in an alternating fashion. The excitation slit width was 2 nm, the emission slit width 6 nm, and the spectrometer time constant 1 s. Measurements were conducted at 295 K. The three repetitions were analyzed independently, and the experimental errors were obtained according to the method described in ref 32. The absolute MFE, χ_{SS} , was evaluated from

$$\chi_{\text{SS}} = \frac{\bar{I}(\lambda_{\text{em}}, B_{\text{sat}}) - \bar{I}(\lambda_{\text{em}}, B_0)}{\bar{I}(\lambda_{\text{em}}, B_0) - (\bar{I}_{\text{F}}(\lambda_{\text{em}}, B_0) - \overline{\text{BG}}(\lambda_{\text{em}}))I_{\text{c}}/I_0 - \overline{\text{BG}}(\lambda_{\text{em}})} \quad (3)$$

Here, $\bar{I}(\lambda_{\text{em}}, B_{\text{sat}})$ and $\bar{I}(\lambda_{\text{em}}, B_0 = 0)$ are the mean intensities at λ_{em} in a saturated magnetic field ($B_{\text{sat}} = 62$ mT) and in the absence of an additional magnetic field, respectively. $\bar{I}_{\text{F}}(\lambda_{\text{em}}, B_0)$ is the residual emission of the locally excited fluorophore at λ_{em} in the absence of quencher. I_{c} and I_0 are the intensities of prompt emission of the fluorophore in the presence and absence of the quencher, respectively, which have been obtained from the decomposition of the fluorescence spectra. $\overline{\text{BG}}(\lambda_{\text{em}})$ is the mean background intensity.

Time-Resolved MFE Measurements and Modeling. Time-resolved data of the MFEs on the exciplex were obtained by the TCSPC technique. In order to investigate the effect of an external magnetic field on the exciplex emission (Figure 1), a saturating magnetic field ($B_0 = 62$ mT) was applied. The fluorophore is excited at 374 nm by a laser diode (Picoquant, LDH-P-C-405), and a 550 nm long-pass filter in front of the detector ensured that only the exciplex luminescence was detected. A detailed description of the experimental setup is given in refs 1 and 2.

The raw data of a typical time-resolved MFE measurement are shown in Figure 1. The time traces rise with a time constant of approximately 2 ns, almost independent of the magnetic field intensity. The decay kinetics of the exciplex emission includes the dissociation into free ions and recombination giving rise to delayed exciplex emission. The time-resolved MFE (TR-MFE) is given as the difference in the exciplex emission intensity,

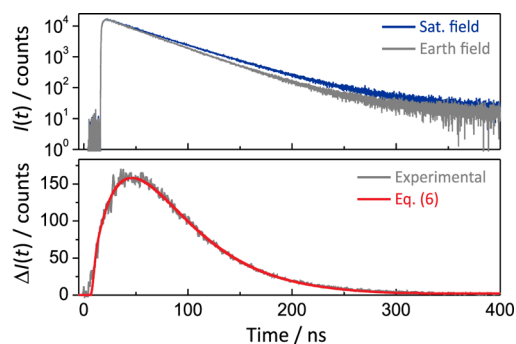


Figure 1. Time-resolved exciplex emission (upper panel) of the 9,10-dimethylantracene (1.5×10^{-5} M)/*N,N*-dimethylaniline (0.06 M) system in a TO/DMSO mixture at $\epsilon_s = 7.3$ in the absence (gray) and presence (blue) of an external magnetic field (62 mT) monitored with a long-pass filter (LP550) after pulsed excitation at 374 nm. In the presence of an external magnetic field, the delayed emission of the exciplex is enhanced. The time evolution of the magnetic field effect $\Delta I(t)$ (lower panel) was obtained by taking the difference of the exciplex emission time traces in the absence and presence of an external magnetic field. The red solid line is calculated from the model, eq 6. In the lower panel, $t = 0$ ns coincides with the pulse excitation; in the upper panel, the emission traces are shifted by approximately 15 ns to longer times.

$\Delta I(t)$, in the absence and presence of the external, biasing magnetic field:

$$\Delta I(t) = I(t, B_0) - I(t, B_0 = 0) \quad (4)$$

In order to determine the MFE, the amplitudes within the first nanosecond after the excitation pulse were matched. We integrated the time traces so obtained to determine the steady-state MFE of the exciplex, χ_{TR} , from the time-resolved MFE measurements:

$$\chi_{\text{TR}} = \frac{\int_0^\infty \Delta I(t) dt}{\int_0^\infty I(t, B_0 = 0) dt} \quad (5)$$

Scheme 1b shows the pertinent reaction pathways for fluorescence quenching by electron transfer. The abscissa can be expressed as the projection of a two-dimensional reaction coordinate comprising the distance between the fluorophore and the quencher and the outer-sphere electron transfer reaction coordinate.^{1,2} The ordinate corresponds to the free energy. An increase in the intensity of the exciplex emission (6) is due to the enhancement of the population of the singlet RIP, which can reform the exciplex via (4). The singlet RIP can be indirectly generated via exciplex dissociation (3), e.g., following a quenching reaction yielding the exciplex (2A), or directly, via a remote electron transfer reaction (2B). Note that the ET reactions preserve the overall spin of the reactant pair; i.e., both the exciplex and the RIP are formed as singlet entities. The external magnetic field gives rise to an increase in the singlet RIP probability and hence the exciplex via pathway 4. As a consequence of the exciplex dissociation here being a slow process, the MFEs generated by the direct ET route (2B) will be observed on a faster time scale than those formed by the exciplex route (2A). In this way, time-resolved MFEs of the exciplex emission can distinguish the reaction channels populating the magneto-sensitive RP state (2B versus 2A).

To simulate the experimental data, we used the model introduced in ref 2. In this model, both initial quenching

products (exciplex or RIP) are possible. The probability that the radical pair system exists as an exciplex, $\rho_E(t, B_0)$, is given by

$$\begin{aligned} \rho_E(t, B_0) = & \phi_E + \phi_1 R(t, B_0 | r_1) \\ & + k_d \int_0^t \rho_E(\tau) R(t - \tau, B_0 | r_E) d\tau \\ & - (k_d + \tau_E'^{-1}) \int_0^t \rho_E(\tau) d\tau \end{aligned} \quad (6)$$

where ϕ_1 is the probability that the RIP is initially generated (pathway 2B in Scheme 1b), k_d denotes the rate constant of exciplex dissociation, r_1 is the distance of RIP formation via distant ET, and $R(t, B_0 | r_1)$ is the probability that a RIP formed at distance r_1 at $t = 0$ has recombined by time t . r_E refers to the contact distance of the fluorophore and quencher, at which the transition of the RIP to the exciplex (or contact ion pair) occurs. $\phi_E = 1 - \phi_1$ is the initial exciplex probability (pathway 2A in Scheme 1b), and τ_E' is the intrinsic exciplex lifetime (without dissociation). The contributions to the exciplex probability in eq 6 can be described as follows: The first term is the probability that the exciplex is formed initially, while the second term accounts for the probability that the initially generated RIP reforms an exciplex at t . The third term describes the probability that the exciplex dissociated at time τ is reformed at t , and the last term models the depopulation of the exciplex by dissociation (k_d) and radiative/nonradiative decay with the rate constant $\tau_E'^{-1}$. $R(t, B_0 | r_1)$ is field dependent and has been calculated in the low-viscosity limit as described in detail in refs 1 and 2. The radical pair was assumed to diffuse in a potential of mean force approximately accounting for the microheterogeneous environment. This potential was calculated following an approach based on the $D-E_0$ theorem as outlined in refs 18 and 20. Note that more elaborate schemes of treating the diffusion-influenced reversible exciplex kinetics have been derived on the basis of the integral encounter theory.^{39–42} While also comprehensively applicable to highly viscous mixtures, this approach is difficult to employ for radical pairs with a multitude of magnetic nuclei (as is the case here) and beyond the scope of the current presentation. Figure 2 illustrates the microheterogeneous medium structure to clarify typical length scales and the extent of the local enrichment of the polar component as predicted on the basis of the continuum model from ref 20.

III. RESULTS AND DISCUSSION

Figure 3 illustrates the dependence of the MFE of the DMAnt/DMA system on the solvent dielectric constant, ϵ_s , of the microheterogeneous TO/DMSO mixture as determined from steady-state (χ_{SS}) and time-resolved (χ_{TR}) measurements (upper panel). The lower panel gives a comparison of the ϵ_s dependence for the binary solvent mixtures of PA/BN (homogeneous) and TO/DMSO (microheterogeneous). Steady-state and time-resolved measurements agree within experimental error. This observation suggests that in both types of experiments the same photochemical reactions are probed. In fact, in view of the low light intensities and low concentrations employed in these experiments, bulk processes such as F-pair reactions and processes involving fluorophore triplets (triplet–triplet and triplet–doublet pair reactions) are not expected to contribute to the observed MFEs here. Instead, the MFEs on the exciplex result exclusively from the effect of an external magnetic field on the S/T mixing in the geminate

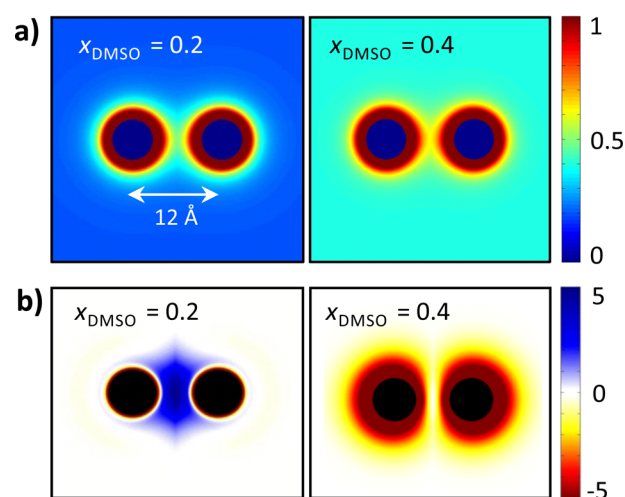


Figure 2. Illustration of the structure of the microheterogeneous solvent surrounding a radical ion pair (contact distance: 6.8 Å) as predicted by the continuum solvation model described in ref 18. (a) Local mole fraction of DMSO in DMSO/toluene mixtures of bulk concentration $x_{\text{DMSO}} = 0.2$ (left; $\epsilon_s = 7.3$) and 0.4 (right; $\epsilon_s = 13$). (b) Deviation of the local dielectric constant from the macroscopic dielectric constant for the two solvent mixtures from part a. The plots show contours through a plane containing the two radical centers. The parameter values as given in ref 20 have been used.

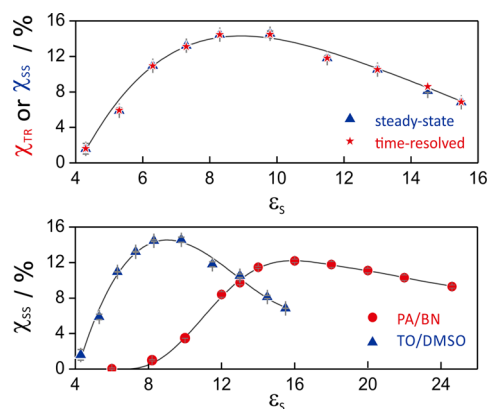


Figure 3. Solvent permittivity dependence of the magnetic field effect of the 9,10-dimethylanthracene/*N,N*-dimethylaniline exciplex determined from steady-state (blue filled triangles) and time-resolved MFE (red filled stars with barely visible error bars reflecting the statistical error of the registration process) measurements in solvent mixtures of TO/DMSO (upper panel). The lower panel compares the MFE in the homogeneous and microheterogeneous solvent mixtures.

radical pair. The onset of the MFE is found at $\epsilon_s = 6$ (with $\chi = 0.1\%$) and $\epsilon_s = 4.3$ (with $\chi = 1.6\%$) in the PA/BN and TO/DMSO mixture, respectively. In the homogeneous PA/BN mixtures, the MFE is small for $\epsilon_s < 10$ but rises sharply for $\epsilon_s \sim 13$ to attain its maximum value around $\epsilon_s \sim 18$ (11%). For larger solvent polarities, it decreases slightly as a larger population of the radical pairs dissociates indefinitely without reencountering (within the coherence time of the radical pair). In the microheterogeneous TO/DMSO mixtures, the onset of the MFE occurs at a lower bulk permittivity and the maximal value (14.5%) is already observed at $\epsilon_s = 8.3$. In essence, the MFE appears to report a more polar environment than would be expected on the basis of the bulk permittivity. These peculiarities in the MFEs can be explained on the basis of a

dielectric enrichment of the polar component (DMSO) in the vicinity of the magneto-sensitive RIP. As a consequence, the effective dielectric constant, ϵ_{eff} of the enriched solvation shell is increased over the bulk dielectric constant, ϵ_s .^{19,20} This specific solvation increases the reencounter probability of the geminate RP without impeding the spin-conversion by too tight binding, which in homogeneous solvents of low polarity is seen to hamper the MFE by confining the radical pairs to configurations with large exchange coupling. As a consequence, larger MFEs are possible in the microheterogeneous environments as compared to homogeneous solutions.

For various dielectric constants, the time-resolved MFEs are shown in Figure 4 together with least-squares fits applying the

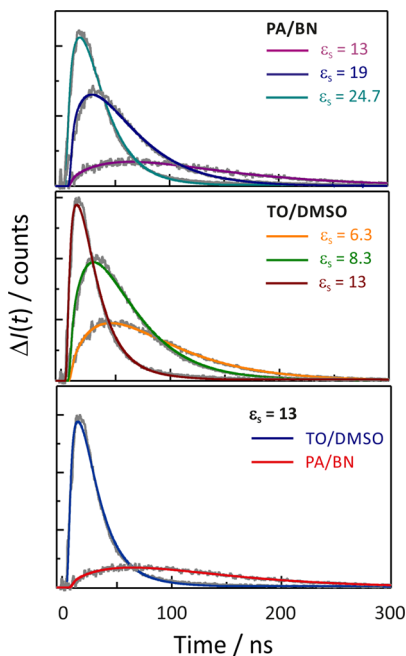


Figure 4. Experimental time-dependent magnetic field effects (ΔI) at different dielectric constants, ϵ_s , in PA/BN (top panel) and TO/DMSO (middle panel) solvent mixtures for the system 9,10-dimethylanthracene/*N,N*-dimethylaniline. The bottom panel compares the TR-MFEs of the exciplex in PA/BN and TO/DMSO mixtures of the same dielectric constant ($\epsilon_s = 13$). The gray and solid colored lines refer to experiment and simulation, respectively.

model given by eq 6. The maximum of the TR-MFEs occurs in the range from 10 to 75 ns after photoexcitation, with larger values occurring at lower dielectric constants. For all samples, the MFEs reached the noise level of the experiment within 400 ns after excitation.

The exciplex lifetime, τ_E , is one of the central parameters characterizing the time evolution of the MFE. We have determined τ_E from the initial decay of the TCSPC traces of the exciplex, for which the RP recombination is negligible. Figure 5 shows that the apparent exciplex lifetime decreases with increasing bulk dielectric constant, ϵ_s , in both binary solvent mixtures. Furthermore, as expected in view of the above discussion, the exciplex lifetimes are considerably smaller in the TO/DMSO mixtures as compared to the iso-bulk dielectric PA/BN mixtures. Note also that the exciplex is an excited charge-transfer complex with correspondingly large dipole moment. As a consequence, its formation is expected to enhance the diffusive enrichment of polar solvent molecules in

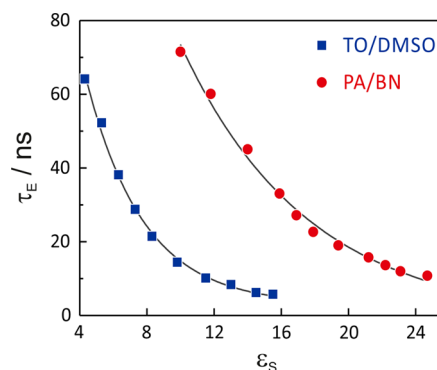


Figure 5. Permittivity dependence of the exciplex lifetimes of the 9,10-dimethylanthracene/*N,N*-dimethylaniline exciplex in PA/BN (red circles) and TO/DMSO mixtures (blue squares). The solid lines have been added to guide the eye.

its surrounding. In this way, the exciplex can act as a catalyst to its own dissociation (pathway 3 in Scheme 1b). As the exciplex lifetime is considerably larger than the characteristic time of solvation, these dynamic aspects can however not be resolved here.

The exciplex kinetics are also characterized by the association constant $K_a = k_a/k_d$ (top panel in Figure 6) and the exciplex

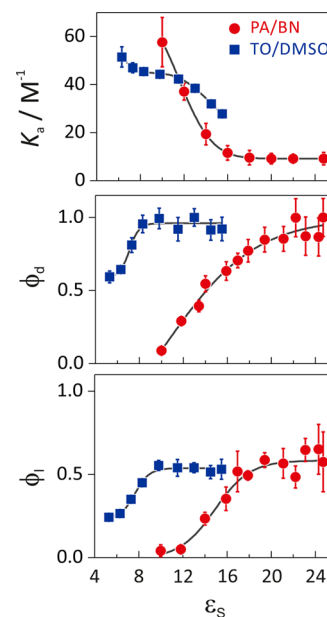


Figure 6. Dependence of the association constant, K_a , the dissociation quantum yield of the exciplex, ϕ_d , and the initial RIP formation, ϕ_i , on the dielectric constants, ϵ_s , of homogeneous (PA/BN) and microheterogeneous (TO/DMSO) solvent mixtures. The filled circles and squares with error bars have been determined from the experimental data by modeling the TR-MFE. The solid lines have been added to guide the eye.

dissociation quantum yield $\phi_d = k_d\tau_E$ (middle panel in Figure 6). ϕ_d was estimated from the dependence of τ_E on dielectric constants assuming that the intrinsic, radiative and nonradiative decay rates are independent of solvent composition. K_a has a strong effect on the shape, i.e., the temporal evolution, of the time-resolved MFEs and can thus be extracted from the experimental data by least-squares fitting.^{1,2} Following this approach as detailed in ref 2, K_a and ϕ_d were obtained as a

function of ϵ_s . In general, ϕ_d increases with ϵ_s , likely because polar environments reduce the exciplex stabilization free energy by increasing the reorganization energy.^{7,32} This effect is indeed found and much more pronounced in the microheterogeneous environment as compared to the homogeneous one. For TO/DMSO, the exciplex dissociation quantum yield approaches $\phi_d = 1$ for a bulk dielectric constant as low as $\epsilon_s = 8$, while for PA/BN mixtures this is only the case at $\epsilon_s \sim 22$.

Likewise, the association constant K_a is expected to decrease with polarity, as is clearly evidenced in Figure 6 for the homogeneous PA/BN solutions. While K_a in general also decreases with increasing polarity for TO/DMSO, it is nearly constant in the range from $\epsilon_s = 8$ to 12. This surprising behavior suggests that k_a increases in this region in parallel to k_d such that K_a is approximately constant. This can likely be attributed to an increased association rate brought about by the microheterogeneous solvation impeding the separation of the radical ions with respect to the homogeneous environment.

Just as K_a , the probability of the initial RIP formation, ϕ_1 , governs the time evolution of MFEs of the exciplex and was extracted from the experimental data by least-squares fitting.^{1,2} The extracted ϕ_1 values are also shown in Figure 6 as a function of the dielectric constant. The data reveal that, for the DMant/DMA system with moderate free energy of charge separation ($\Delta G_{et} = -0.28$ eV),^{43,44} the direct exciplex formation (pathway 2A in Scheme 1b) contributes at all dielectric constants in homogeneous and microheterogeneous environments. Furthermore, the probability of distant ET quenching increases with increasing solvent polarity. Note that the requirement to detect the exciplex luminescence limits the accessible ϵ_s range to the indicated range; beyond the respective limits, the exciplex emission is insufficient for the accurate determination of ΔI . In both solvent mixtures, ϕ_1 levels off at $\phi_1 = 0.55$. For TO/DMSO, this is the case for $\epsilon_s \geq 9$, and for PA/BN, for $\epsilon_s \geq 20$, in agreement with the general bearing. Distant electron transfer quenching is more favored in polar solutions, where it leads to a better solvation of the reaction products (RIPs). This holds true despite a minor increase in the reorganization energy resulting from the increasing polarity. In the low-viscous solutions studied here, the diffusive approach of the reactants is fast enough compared to the intrinsic electron transfer rate to always form a contact complex (exciplex) at the contact distance. As a consequence, ϕ_1 is smaller than unity, even for the most polar and hardly emissive solutions.

IV. CONCLUSIONS

In this work, we have employed time-resolved MFE measurements to study the exciplex and RIP dynamics of the DMant/DMA system in homogeneous and microheterogeneous solvent mixtures of various bulk permittivities. We use a model accounting for the reversible exciplex dissociation to identify the peculiarities resulting from microheterogeneous solvent environments in solvent mixtures of TO and DMSO. The exciplex dynamics and the initial quenching products depend strongly on the solvent properties. In microheterogeneous solvents, specific solvation of the exciplex and RIP gives rise to an environment that is significantly more polar than that observed in homogeneous solvents of comparable bulk permittivity. For low permittivities, this brings about a larger dissociation quantum yield of the exciplex, a lower exciplex lifetime, and a larger probability that the system undergoes distant electron transfer quenching. Specific solvation furthermore impedes the radical separation such that, in the

permittivity region from 7 to 15, the association constant decays only slowly with the solvent polarity in the TO/DMSO mixtures. In both environments, the probability of the initial formation of RIPs is always less than unity; i.e., the exciplex formation contributes at all ϵ_s . In microheterogeneous solution, the local concentration of DMSO in the solvation shell around the exciplexes and RIPs plays an important role in the exciplex kinetics and the fluorescence quenching mechanism. Together with earlier works, this study demonstrates that time-resolved MFE studies have the potential to provide detailed insights into the reaction dynamics of RIPs and exciplexes. Since the reaction dynamics of the geminate radical pair are very sensitive to small changes in the local dielectric environment, the technique is here recognized as a versatile tool in revealing and characterizing the phenomenon of specific solvation in solvent mixtures.

AUTHOR INFORMATION

Corresponding Author

*E-mail: daniel.kattmig@chem.ox.ac.uk

ORCID

Daniel R. Kattmig: 0000-0003-4236-2627

Notes

The authors declare no competing financial interest.

ACKNOWLEDGMENTS

Financial support from the Vietnam International Education Development (VIED, project 322) and the Austrian Science Foundation (FWF-Project P 21518-N19) is gratefully acknowledged. D.R.K. thanks Dr. Sabine Richert (University of Oxford) for helpful comments.

REFERENCES

- (1) Hoang, H. M.; Pham, T. B. V.; Grampp, G.; Kattmig, D. R. Exciplexes versus Loose Ion Pairs: How Does the Driving Force Impact the Initial Product Ratio of Photoinduced Charge Separation Reactions? *J. Phys. Chem. Lett.* **2014**, *5* (18), 3188–3194.
- (2) Richert, S.; Rosspeintner, A.; Landgraf, S.; Grampp, G.; Vauthey, E.; Kattmig, D. R. Time-Resolved Magnetic Field Effects Distinguish Loose Ion Pairs from Exciplexes. *J. Am. Chem. Soc.* **2013**, *135* (40), 15144–15152.
- (3) Leonhardt, H.; Weller, A. Electron Transfer Reactions of Excited Perylenes. *Berichte Bunsenges. Für Phys. Chem.* **1963**, *67* (8), 791–795.
- (4) Mataga, N. Photochemical Charge Transfer Phenomena - Picosecond Laser Photolysis Studies. *Pure Appl. Chem.* **1984**, *56* (9), 1255–1268.
- (5) Hui, M.-H.; Ware, W. R. Exciplex Photophysics. V. The Kinetics of Fluorescence Quenching of Anthracene by N,N-Dimethylaniline in Cyclohexane. *J. Am. Chem. Soc.* **1976**, *98* (16), 4718–4727.
- (6) Van Haver, P.; Helsen, N.; Depaemelaere, S.; Van der Auwaer, M.; De Schryver, F. C. The Influence of Solvent Polarity of the Nonradiative Decay of Exciplexes. *J. Am. Chem. Soc.* **1991**, *113* (18), 6849–6857.
- (7) Murata, S.; Tachiya, M. Unified Interpretation of Exciplex Formation and Marcus Electron Transfer on the Basis of Two-Dimensional Free Energy Surfaces. *J. Phys. Chem. A* **2007**, *111* (38), 9240–9248.
- (8) Murata, S.; Tachiya, M. Transient Effect in Fluorescence Quenching by Electron Transfer. 3. Distribution of Electron Transfer Distance in Liquid and Solid Solutions. *J. Phys. Chem.* **1996**, *100* (10), 4064–4070.
- (9) Mataga, N.; Chosrowjan, H.; Taniguchi, S. Ultrafast Charge Transfer in Excited Electronic States and Investigations into Fundamental Problems of Exciplex Chemistry: Our Early Studies and Recent Developments. *J. Photochem. Photobiol., C* **2005**, *6* (1), 37–79.

- (10) Koch, M.; Letrun, R.; Vauthey, E. Exciplex Formation in Bimolecular Photoinduced Electron-Transfer Investigated by Ultrafast Time-Resolved Infrared Spectroscopy. *J. Am. Chem. Soc.* **2014**, *136* (10), 4066–4074.
- (11) Koch, M.; Licari, G.; Vauthey, E. Bimodal Exciplex Formation in Bimolecular Photoinduced Electron Transfer Revealed by Ultrafast Time-Resolved Infrared Absorption. *J. Phys. Chem. B* **2015**, *119* (35), 11846–11857.
- (12) Mohammed, O. F.; Adamczyk, K.; Banerji, N.; Dreyer, J.; Lang, B.; Nibbering, E. T. J.; Vauthey, E. Direct Femtosecond Observation of Tight and Loose Ion Pairs upon Photoinduced Bimolecular Electron Transfer. *Angew. Chem., Int. Ed.* **2008**, *47* (47), 9044–9048.
- (13) Petrov, N. K.; Wiessner, A.; Staerk, H. A Simple Kinetic Model of Preferential Solvation in Binary Mixtures. *Chem. Phys. Lett.* **2001**, *349* (5–6), 517–520.
- (14) Petrov, N. K.; Wiessner, A.; Fiebig, T.; Staerk, H. Study of Preferential Solvation in Binary Solvent Mixtures by the Spectro-Streak Picosecond Technique. *Chem. Phys. Lett.* **1995**, *241* (1–2), 127–132.
- (15) Petrov, N. K.; Borisenko, V. N.; Starostin, A. V.; Al'fimov, M. V. Polar Molecular Clusters Produced upon Photoinduced Electron Transfer in an Intermolecular Exciplex in Binary Solvents. *J. Phys. Chem.* **1992**, *96* (7), 2901–2903.
- (16) Petrov, N. K.; Shushin, A. I.; Frankevich, E. L. Solvent Effect on Magnetic Field Modulation of Exciplex Fluorescence in Polar Solutions. *Chem. Phys. Lett.* **1981**, *82* (2), 339–343.
- (17) Basilevsky, M.; Odinkov, A.; Nikitina, E.; Grigoriev, F.; Petrov, N.; Al'fimov, M. Advanced Dielectric Continuum Model of Preferential Solvation. *J. Chem. Phys.* **2009**, *130* (2), 024505.
- (18) Basilevsky, M. V.; Odinkov, A. V.; Nikitina, E. A.; Petrov, N. C. The Dielectric Continuum Solvent Model Adapted for Treating Preferential Solvation Effects. *J. Electroanal. Chem.* **2011**, *660* (2), 339–346.
- (19) Pal, K.; Kattinig, D. R.; Grampp, G.; Landgraf, S. Experimental Observation of Preferential Solvation on a Radical Ion Pair Using MARY Spectroscopy. *Phys. Chem. Chem. Phys.* **2012**, *14* (9), 3155–3161.
- (20) Pal, K.; Grampp, G.; Kattinig, D. R. Solvation Dynamics of a Radical Ion Pair in Micro-Heterogeneous Binary Solvents: A Semi-Quantitative Study Utilizing MARY Line-Broadening Experiments. *ChemPhysChem* **2013**, *14* (14), 3389–3399.
- (21) Steiner, U. E.; Ulrich, T. Magnetic Field Effects in Chemical Kinetics and Related Phenomena. *Chem. Rev.* **1989**, *89* (1), 51–147.
- (22) Closs, G. L. Mechanism Explaining Nuclear Spin Polarizations in Radical Combination Reactions. *J. Am. Chem. Soc.* **1969**, *91* (16), 4552–4554.
- (23) Salikhov, K. M.; Molin, I. N.; Buchachenko, A. L. *Spin Polarization and Magnetic Effects in Radical Reactions*; Akadémiai Kiadó: Budapest, Hungary, 1984.
- (24) Hayashi, H. *Introduction to Dynamic Spin Chemistry: Magnetic Field Effects on Chemical and Biochemical Reactions*; World Scientific Publishing Company: River Edge, NJ, 2004.
- (25) Kaptein, R.; Oosterhoff, J. L. Chemically Induced Dynamic Nuclear Polarization II. *Chem. Phys. Lett.* **1969**, *4* (4), 195–197.
- (26) Rodgers, C. T.; Norman, S. A.; Henbest, K. B.; Timmel, C. R.; Hore, P. J. Determination of Radical Re-Encounter Probability Distributions from Magnetic Field Effects on Reaction Yields. *J. Am. Chem. Soc.* **2007**, *129* (21), 6746–6755.
- (27) Henbest, K. B.; Kukura, P.; Rodgers, C. T.; Hore, P. J.; Timmel, C. R. Radio Frequency Magnetic Field Effects on a Radical Recombination Reaction: A Diagnostic Test for the Radical Pair Mechanism. *J. Am. Chem. Soc.* **2004**, *126* (26), 8102–8103.
- (28) Aich, S.; Basu, S. Magnetic Field Effect: A Tool for Identification of Spin State in a Photoinduced Electron-Transfer Reaction. *J. Phys. Chem. A* **1998**, *102* (4), 722–729.
- (29) Justinek, M.; Grampp, G.; Landgraf, S.; Hore, P. J.; Lukzen, N. N. Electron Self-Exchange Kinetics Determined by MARY Spectroscopy: Theory and Experiment. *J. Am. Chem. Soc.* **2004**, *126* (17), 5635–5646.
- (30) Lukzen, N. N.; Kattinig, D. R.; Grampp, G. The Effect of Signs of Hyperfine Coupling Constant on MARY Spectra Affected by Degenerate Electron Exchange. *Chem. Phys. Lett.* **2005**, *413* (1–3), 118–122.
- (31) Kattinig, D. R.; Rosspeintner, A.; Grampp, G. Fully Reversible Interconversion between Locally Excited Fluorophore, Exciplex, and Radical Ion Pair Demonstrated by a New Magnetic Field Effect. *Angew. Chem., Int. Ed.* **2008**, *47* (5), 960–962.
- (32) Kattinig, D. R.; Rosspeintner, A.; Grampp, G. Magnetic Field Effects on Exciplex-Forming Systems: The Effect on the Locally Excited Fluorophore and Its Dependence on Free Energy. *Phys. Chem. Chem. Phys.* **2011**, *13* (8), 3446–3460.
- (33) Nath, D. N.; Chowdhury, M. Effect of Variation of Dielectric Constant on the Magnetic Field Modulation of Exciplex Luminescence. *Pramana* **1990**, *34* (1), 51–66.
- (34) Petrov, N. K.; Markov, D. E.; Gulakov, M. N.; Al'fimov, M. V.; Staerk, H. Study of Preferential Solvation in Binary Mixtures by Means of Frequency-Domain Fluorescence Spectroscopy. *J. Fluoresc.* **2002**, *12* (1), 19–24.
- (35) Roy, P.; Jana, A. K.; Das, D.; Nath, D. N. Study of Magnetic Field Effect on Py-DMA Exciplex Luminescence in THF–DMF Binary Solvents: Evidence of Multiple Exciplex Formation at Higher Bulk Dielectric Constant. *Chem. Phys. Lett.* **2009**, *474* (4–6), 297–301.
- (36) Jana, A. K. Further Studies on Relaxed and Un-Relaxed Exciplexes in Pyrene-N,N-Dimethylaniline System in Benzene-Acetonitrile Binary Solvents. *J. Phys. Chem. Biophys.* **2015**, *5* (6), 1000194.
- (37) Marcus, R. A. On the Theory of Oxidation-Reduction Reactions Involving Electron Transfer. I. *J. Chem. Phys.* **1956**, *24* (5), 966–978.
- (38) Marcus, R. A.; Sutin, N. Electron Transfers in Chemistry and Biology. *Biochim. Biophys. Acta, Rev. Bioenerg.* **1985**, *811* (3), 265–322.
- (39) Burshtein, A. I.; Ivanov, A. I. Diffusion Affected Magnetic Field Effect in Exciplex Fluorescence. *J. Chem. Phys.* **2014**, *141* (2), 024508.
- (40) Feskov, S. V.; Burshtein, A. I.; Ivanov, A. I. Magnetic Field Effects in Fluorescence of Exciplex and Fluorophore for the Weller Schemes I and II: Similarities and Differences. *J. Phys. Chem. C* **2014**, *118* (37), 21365–21376.
- (41) Dodin, D. V.; Ivanov, A. I.; Burshtein, A. I. Hyperfine Interaction Mechanism of Magnetic Field Effects in Sequential Fluorophore and Exciplex Fluorescence. *J. Chem. Phys.* **2013**, *138* (12), 124102.
- (42) Dodin, D. V.; Ivanov, A. I.; Burshtein, A. I. Magnetic Field Effect in Fluorescence of Excited Fluorophore Equilibrated with Exciplex That Reversibly Dissociates into Radical-Ion Pair Undergoing the Spin Conversion. *J. Chem. Phys.* **2012**, *137* (2), 024511.
- (43) Kavarnos, G. J. *Fundamentals of Photoinduced Electron Transfer*; VCH Publishers: New York, 1993.
- (44) Montalti, M.; Murov, S. L. *Handbook of Photochemistry*; CRC/Taylor & Francis: Boca Raton, FL, 2006.